Melting layer characterization and identification with a C-band dual-polarization radar : a long-term analysis.

Pierre Tabary[1], Alain Le Henaff[1], Gianfranco Vulpiani[1], Jacques Parent-du-Châtelet[1] and Jonathan J. Gourley[2]

[1] Météo-France, DSO, Centre de Météorologie Radar, Trappes, France

[2] NOAA/National Severe Storms Laboratory, Norman, OK (USA)

1 Introduction

Bright band has always been recognized as a major source of error in radar Quantitative Precipitation Estimation (QPE) especially in the winter time (Zawadzski 1984). Many operational services have introduced real-time Vertical Profile of Reflectivity identification and correction procedures (e.g. Koistinen 1991). However, bright band is not always easy to recognize on conventional reflectivity images because of the large variability of the horizontal reflectivity field and because of beam smoothing. Dual-polarization clearly offers new perspectives in that regard (Brandes and Ikeda 2004; Ikeda et al. 2004; Giangrande et al. 2005).

One of the objectives of this paper is to present a long-term characterization of the vertical profiles of Z_H, Z_{DR}, Φ_{DP} and ρ_{HV} observed during stratiform events with the new French operational C-band dual-polarization located in Trappes, near Paris. This radar was installed in March 2004 in the frame of the French PANTHERE radar (Parent-du-Châtelet and Guimera 2003; Gourley et al. 2006a) and has been operating continuously since then. Based on that climatology, conceptual models of vertical profiles of Z_H, Z_{DR}, Φ_{DP} and ρ_{HV} are proposed and a robust identification algorithm is developed and tested.

2 A long-term melting layer characterization

Twenty episodes of stratiform precipitation were selected over the period December 2004 – March 2006. The retrieval of the vertical profile of polarimetric variables was carried out using only the 9° tilt, which the highest "almost horizontal" tilt of the Trappes Volume Coverage Pattern.

That tilt is revisited every 15 minutes. The Trappes Volume Coverage Pattern also includes a 90° tilt but it is essentially used to calibrate Z_{DR}. Radar data at 9° were corrected for ground-clutter and other non-precipitating echoes using a fuzzy logic algorithm (Gourley et al. 2006b). Care was taken not to remove the bright band signature, which, as will be seen later, share some common characteristics – in terms of ρ_{HV} and textures – with ground clutter. Low-SNR data (less than 10 dB) were flagged and subsequently removed. Values of correlation coefficient were corrected for low-SNR bias. Differential reflectivity was corrected for a system bias (-0.08 dB for Trappes, see Gourley et al. 2006a) and Φ_{DP} for the system differential phase (-6.5°) and azimuthal interferences. Likewise, only pixels having a reflectivity above 10 dBZ were considered. The vertical profile of each variable (Z_H, Z_{DR}, Φ_{DP} and ρ_{HV}) was then obtained by averaging the remaining quality-controlled data across all azimuths. The estimation of the mean at a given height was validated if at least one fourth (i.e. 180) of the pixels were available. Time series of vertical profiles were then constructed. Whenever it was relevant (i.e. no significant variation of the bright band height, thickness, … was observed) the mean ± standard deviation of the profile was computed over the entire episode. The profiles of horizontal and differential reflectivity were first normalized by the value at low levels so as to allow comparison between profiles associated with different low-level intensity.

Figure 1 shows PPIs of Z_H, Z_{DR}, ρ_{HV} and Φ_{DP} obtained on the 17 December 2004 at 07 UTC. All PPIs show a well-defined circular ring, which obviously corresponds to the bright band. Figure 2 shows the mean ± standard deviation profiles over the entire episode. Figure 2 is very similar to the profiles obtained from S-POL RHI measurements by Brandes and Ikeda (2004). The 0°C height

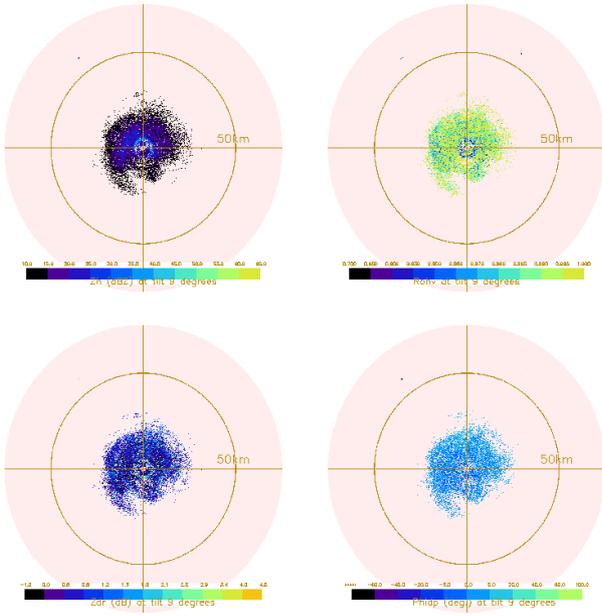measured by commercial aircrafts over the period has been superimposed.

Figure 1 : PPIs of Z_H, Z_{DR}, ρ_{HV} and Φ_{DP} obtained on the 17 December 2004 at 07.00 UTC.
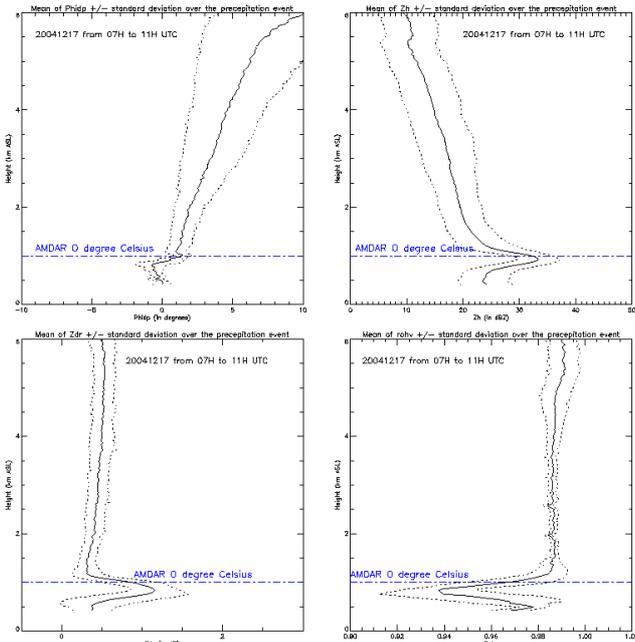

Figure 2: Mean ± standard deviation vertical profiles of Z_H, Z_{DR}, ρ_{HV} and Φ_{DP} obtained on the 17 December 2004.

A careful examination of the 20 retrieved profiles permitted us to draw the following conclusions:

➢ The melting layer signature is located at a similar height for all four polarimetric variables.

➢ ρ_{HV} decreases to 0.93 on average in the middle of the bright band, with values above and below always very stable and above 0.98, independent of the surface

rainfall intensity. This is a remarkable feature of ρ_{HV}, as opposed to Z_H and Z_{DR}, which we take advantage of in the identification algorithm (see Section 3).

➢ Z_H and Z_{DR} are typically increased by 5 and 1 dB, respectively, in the melting layer but the enhancement and the values above and below are quite variable both in space and time.

➢ The Z_{DR} profile always exhibits a positive gradient ($+0.1$ dB km^{-1}) above the melting layer.

Those conclusions lead to conceptual models for the vertical profiles of each polarimetric variable. The conceptual model for ρ_{HV} is given on Fig. 3.
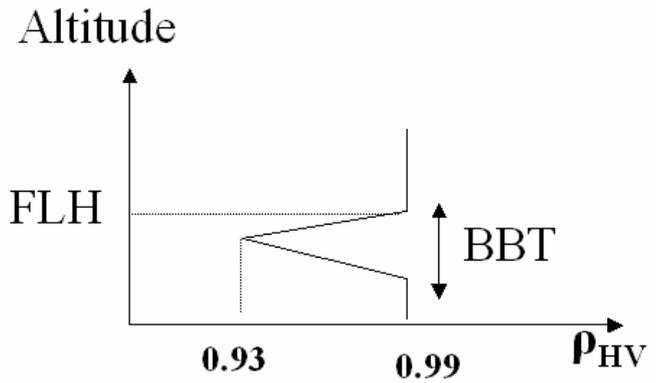

Figure 3: Proposed conceptual model for the vertical profile of ρ_{HV}.

The ρ_{HV} profile is simply defined by two parameters, the Freezing Level Height (FLH) , which determines the top of the melting layer, and the Bright Band Thickness (BBT).

3 Development of the identification algorithm

The proposed identification algorithm is entirely based on ρ_{HV}, which may appear as a recession with respect to previous works (e.g. Brandes and Ikeda 2004). However, we rapidly came to the conclusion that the added value of the other parameters was very small. Besides, as mentioned before, the horizontal variability of Z_H and Z_{DR} quite often blurs the bright band signature and makes them useless for melting layer identification, especially when data from low-elevation angles are considered. The current version of the algorithm assumes that the bright band characteristics (bright band height and bright band thickness) are the same all around the radar. Data gathered at all N elevation angles of the VCP are quality controlled and then averaged – for each range - across all available azimuths to yield a set of N mean radial curves of ρHV ($\rho_{HV}^{OBS}(r)$). Averaging across all

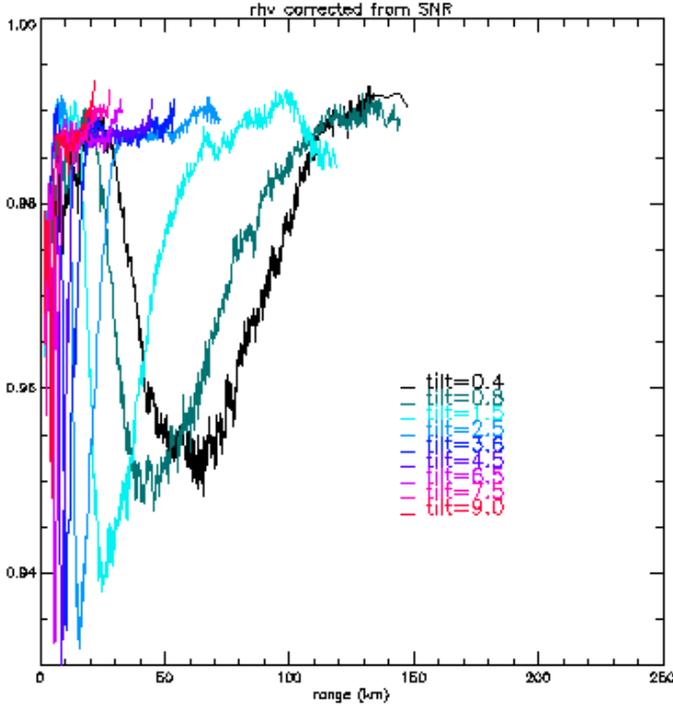azimuths aims at enhancing the bright band signature.

Figure 4 : An example of the set of $\rho_{HV}^{OBS}(r)$ curves obtained at 07.00 UTC on the 17 December 2004.

Figure 4 presents a set of observed $\rho_{HV}^{OBS}(r)$ curves obtained on the 17 December 2004. The bright band is clearly noticeable at all tilts through a decrease of the ρ_{HV} values. However, the location, magnitude and shape of the disturbance changes significantly from tilt to tilt illustrating the effect of beam broadening. The proposed identification algorithm takes that process into account and proceeds as follows:

➢ The true ρ_{HV} profile is assumed to be well-represented by a triangular shape as in Fig. 3. Two parameters – the freezing level height (FLH) and the bright band thickness (BBT) – define the profile.

➢ The two parameters FLH and BBT are varied within a given range. FLH varies from 0 to 4 km with a 200 m increment and BBT from 200 to 1000 m with a 200 m increment.

➢ For each couple (FLH, BBT) a set of simulated radial curves of ρ_{HV} are generated. Going back to the definition of ρ_{HV} and denoting $P(\theta)$ the two-way power antenna diagram, the filtered ρ_{HV} can be expressed as a function of the intrinsic ρ_{HVi}, Z_{Hi} and Z_{Vi} as follows:

ρ_{HV} = $[\Sigma_i P(\theta_i).\rho_{HVi}.\sqrt{(Z_{Hi})}.\sqrt{(Z_{Vi})}]$

/ $[\sqrt{(\Sigma P(\theta_i).Z_{Hi})} . \sqrt{(\Sigma P(\theta_i).Z_{Vi})}]$,

where the summation is done over the antenna diagram and Z_H and Z_V are expressed in linear units. If the intrinsic Z_H and Z_V can be assumed to be constant over the integration range, then the measured ρ_{HV} simply becomes the weighted average of the intrinsic ρ_{HV}, with the weights being given by

the antenna diagram. This calls out for some discussion as it is well known that Z_H and Z_V are varying a lot throughout the bright band (see Fig. 2).

➢ The set of simulated ρ_{HV}^{SIM} radial curves are then compared to the observed ones (ρ_{HV}^{OBS}) and the best (FLH,BBT) couple – in the sense of the correlation between observed and simulated $\rho_{HV}(r)$ curves - is selected.
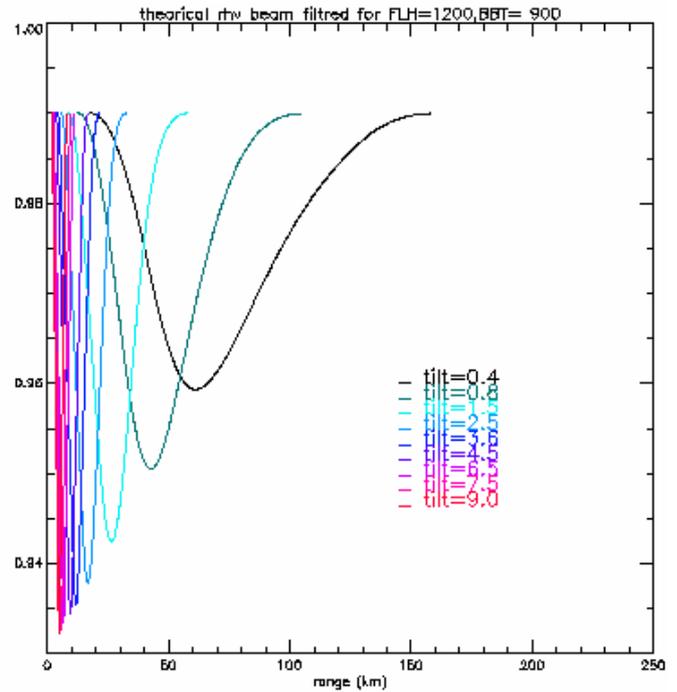

Figure 5 : An example of a set of simulated curves for FLH=1200 m and BBT=900 m , which is the (FLH,BBT) couple that gives the best fit with the observed $\rho_{HV}(r)$ curves presented on Fig. 4.

Figure 5 presents the simulated curves $\rho_{HV}^{SIM}(r)$ obtained with the best candidate (FLH,BBT). The comparison with the set of observed curves shows that the effect of beam broadening is quite well reproduced.

4   Evaluation

The FLH information has been compared to the 0°C isotherm measured routinely by landing and taking-off aircrafts at the Paris airports (so-called AMDAR measurements). It should be mentioned that these data are totally independent from the radar measurements.

Figure 6 is a time series showing the top and bottom of the bright band, as identified by the radar-based algorithm, along with aircraft measurements of the 0°C isotherm (so-called AMDAR measurements). The agreement is excellent, then trend is fairly well reproduced. In the case

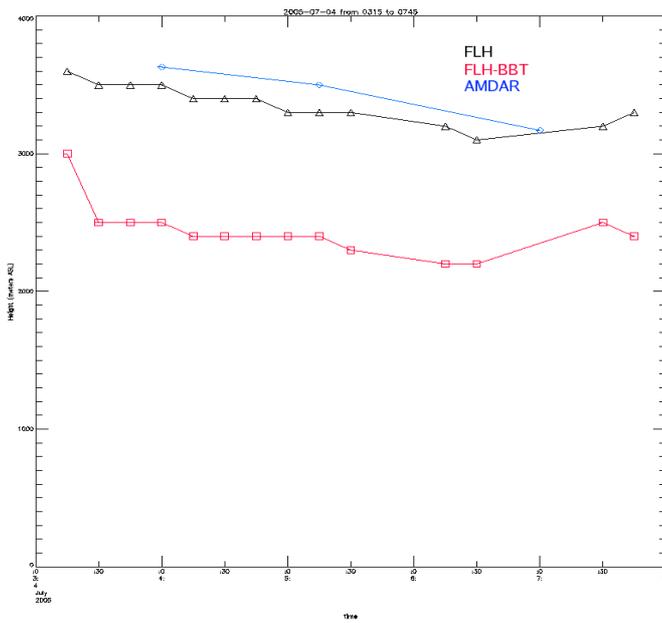that is presented, the radar-based estimation is about 100 – 200 m lower than the aircraft measurements.

Figure 6 : a time series of the FLH and FLH-BBT levels retrieved by the method together with AMDAR measurement on the 4 July 2004.

5   Conclusions and perspectives

The vertical profiles of polarimetric variables (Z_H, Z_{DR}, ρ_{HV} and Φ_{DP}) have been characterized using 20 episodes of stratiform precipitation. The data come from the new French C-band polarimetric radar located in Trappes near Paris. This long-term analysis confirms that the melting layer has a very clear signature on each of the four polarimetric variables. The horizontal and differential reflectivity are typically increased by 5 and 1 dB, respectively. ρ_{HV} drops down to 0.93 (on average) and the differential phase (Φ_{DP}) exhibits an increase of about 10°. Based on that climatology, conceptual models have been proposed for the vertical profiles of each of the four polarimetric variables. An identification algorithm has been developed that is entirely based on ρHV, the enormous advantage of which over Z_H and Z_{DR} is that its values above and below the bright band (0.99) are independent of the low-level intensity. The algorithm assumes that the melting characteristics (height and thickness) are the same all around the radar. It takes into account the effect of beam smoothing, which is a problem that has been very often mentioned but rarely solved (e.g. Brandes and Ikeda 2004). The algorithm has been run on all 20 situations and the top of the identified melting layer has been systematically compared with independent aircraft measurements. Overall, the agreement is excellent, both in terms of correlation and mean difference.

References

Brandes, E.A. and K. Ikeda, 2004: Freezing-level estimartion with polarimetric radar, J. Appl. Meteor., 43, 1541 – 1553.

Giangrande, S. E., A. V. Ryzhkov, and J. Krause, 2005: Automatic detection of the melting layer with a polarimetric prototype of the WSR-88D radar. Preprints, 32nd Conf. on Radar Meteorology, Albuquerque, New Mexico, Amer. Meteor Soc., CD-ROM 11R.2.

Gourley, JJ, P. Tabary, J. Parent-du-Chatelet, 2006a: data quality of the Météo France C-band polarimetric radar, accepted in *J. Atmos. Oceanic Technol.*.

—————, —————, and —————, 2006b: A fuzzy logic algorithm for the separation of precipitating from non-precipitating echoes using polarimetric radar observations. *J. Atmos. Oceanic Technol.* Under review.

Ikeda, K., E.A. Brandes, and R.M. Rasmussen, 2004: Polarimetric Radar Observation of Multiple Freezing Levels, J. Atmos. Sciences, 62, 3624 – 3636.

Koistinen, J., 1991 : Operational correction of radar rainfall errors due to the vertical reflectivity profile. Preprints, 25th *Int. Conf. On Radar Meteorology*, Paris, France, Amer. Meteor. Soc., 91-94.

Parent-du-Châtelet, J., and M. Guiméra, 2003 : The PANTHERE project of Météo France : extension and upgrade of the French radar network, *Proc. 31st Conf. On Radar Meteorology*, Seattle, WA, Amer. Meteor. Soc., 802 – 804.

Tabary, P., 2006 : The new French radar rainfall product. Part I : methodology, submitted to Wea. Forecasting.

Zawadzki, I., 1984: Factors Affecting the Precision of Radar Measurements of Rain. Preprints, 22nd *Conference on Radar Meteorology*, Zurich, Switzerland, Amer. Meteor. Soc., 251-256.